

Beam Deflection with the Aid of a Nonlinear Resonance

M. M. Gordon\*

We heard this morning about beam extraction by more or less standard methods. I would like to describe now what we consider a rather unconventional technique, which we hope will be technically well adapted to these sector machines. It is a modification of the basic regenerative idea of the Tuck, Teng, and LeCouteur scheme wherein we try to make use of nonlinear resonances that occur in these machines. We heard lots of talk yesterday about all of the problems and harrassments that can arise from these resonances, and what I shall point out here is that perhaps we can make use of nonlinear resonances to help us get the beam out of the machine.

Basically the idea is quite simple. The nonlinear resonance has the property that it will build up radial oscillation amplitude in the machine at a rapidly accelerated rate, so that one could in principle get a large turn separation from this effect. However, since these resonances are nonlinear in character their effect is very small for small amplitudes of oscillation and only become significant as the amplitudes get larger. Thus, some sort of additional field bump must be present to start the oscillations off and to drive them up to an amplitude where the nonlinearity can take over and produce a rapidly accelerated growth rate in these radial oscillations. This, then, is the basic idea.

The difficulty with this scheme, as we soon discovered (and which is also the difficulty with the standard deflection technique), is in maintaining axial stability in the process of getting the beam deflected. In this technique the radial oscillation amplitudes are built up to quite sizable amounts, and nonlinear coupling resonances that would ordinarily have small effect come in with increasingly stronger and stronger effect. If these effects persist long enough, they destroy the axial stability of the beam.

In the medium energy cyclotron, the value of  $v_r$  rises above unity as the particles accelerate out from the center, which is all very well for getting away from the nonlinear resonances effects. However, if we want to make use of these effects for beam deflection we must, of course, drive the value of  $v_r$  back toward unity near the outside of the machine. We must tailor the field in some way to accomplish this. First, we should have the average field drop off. In addition, to avoid raising the value of  $v_z$  the flutter field should drop off at the same time which moreover will enhance the drop in  $v_r$ . We want to keep the value of  $v_z$  low, because the large radial oscillations, together with the coupling resonance, will tend to make the value of  $v_z$  rise toward the critical value of 0.5, which should be avoided.

This manipulation of the field will lead to non-isochronous conditions and it will be a problem to get the beam out before there is too much loss of phase. We could tailor the field previous to that so as to gain sufficient phase such that the phase loss during the extraction essentially just brings the beam back past the peak of the voltage wave.

---

\*This work was performed at ORNL during the academic year 1957-58 while the author was on leave from the University of Florida. Present address: Department of Physics and Astronomy, Michigan State University, East Lansing, Michigan.

If possible, what we would like to do, in addition to getting  $\nu_r$  back down to unity, is to manipulate the field in more subtle ways to strengthen the instability arising from the nonlinear radial resonances (either the 3/3 or the 4/4), and at the same time try to tailor these fields to minimize the effects of coupling resonances.

I want to present some calculations relative to this type of deflection scheme which were made specifically for the high energy cyclotron being developed at ORNL. Here the particles are accelerated up to  $\nu_r = 2$ , which in this 8-sector machine I am going to talk about occurred at around 800 Mev. Thus, there is no problem in getting the particle to the resonance. Since it is an 8-sector machine,  $\nu_r = 2$  is an 8/4 cubic nonlinear essential resonance. Although this work does not apply directly to the medium energy cyclotron, it will, I think, point out the sort of procedures one has to go through in order to see whether such a system is feasible in a particular machine.

Figure 229 shows the form of the 8-sector field in the median plane that we put into the computer. It is a weak spiral field in which the spiral angle is just  $r^2$ . The value of the flutter,  $f(r)$ , is adjusted within certain limitations to give a fairly flat  $\nu_z$  energy curve, the value of  $\nu_z$  being about 0.25 in this range. At the bottom of the figure we have the data at the resonance when  $\nu_r = 2$ , or 8/4. The momentum, energy,  $\nu_z$  value, and average radius of the orbit are given here. The cyclotron unit in this machine is about 600 cm, and so the radius of this orbit is about 600 cm, and so the radius of this orbit is about 500 cm. Also  $\tan \alpha$  (sometimes referred to as  $\gamma$ ) is shown and it can be seen that the spiral is quite moderate.

MEDIAN PLANE FIELD: (cyclotron units)

$$B_z = - \frac{1}{\sqrt{1-r^2}} [1 + f(r) \cos 8(\theta - r^2)]$$

WHERE  $f(r) = r^2 + 0.5896 r - 0.1660$

FOR  $\nu_r = 8/4$

$$p = 1.5566 \text{ mc}$$

$$E_K = 0.8502 \text{ mc}^2$$

$$\nu_z = 0.2482$$

$$\bar{r} = 0.8413$$

$$f(\bar{r}) = 1.038$$

$$\tan \alpha = 1.415$$

Fig. 229. Form of 8-sector field in median plane.

Figure 230 shows an outline of the nonlinear resonance theory as it applies to the  $\nu_r = 8/4$  case. To save time we shall not discuss this material. The only thing we should point out right now is that one could anticipate a rise in amplitude which is proportional to the cube of the amplitude if the phase of the oscillation is just right.

In Figure 231 we have the phase plot obtained at the 8/4 resonance. What we did was to put particles in orbits starting out with different amplitudes and phases, and plot once per revolution (once per oscillation actually) the value of  $p_r$  vs  $r$  as obtained from the computer for each value of orbit. What we have in this figure is actually only one-quarter of the total phase space. The particular value in the machine at which this phase plot was recorded was specifically hunted for. The phase points are all moving

APPROXIMATE INVARIANT FOR  $\nu_r = 8/4$  :

$$H(A, \phi) = C_0 A^4 - C_1 A^4 \sin 4\phi$$

RESULTING EQUATIONS OF MOTION :

$$\frac{dA^2}{d\theta} = -\frac{\partial H}{\partial \phi} = 4C_1 A^4 \cos 4\phi$$

$$\frac{d\phi}{d\theta} = \frac{\partial H}{\partial A^2} = 2C_0 A^2 - 2C_1 A^2 \sin 4\phi$$

Fig. 230. Nonlinear resonance theory applied to  $\nu_r = 8/4$ .

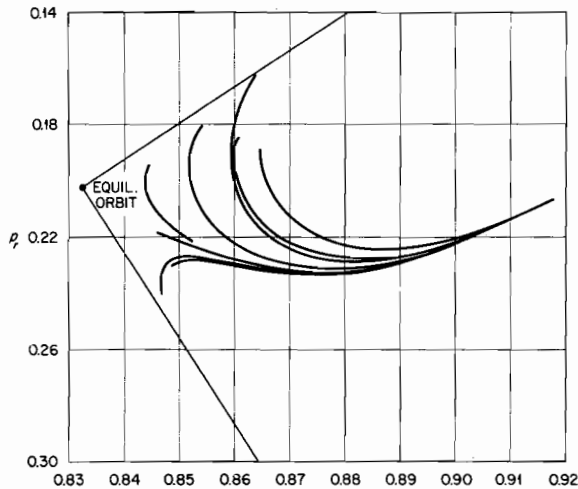


Fig. 231. Phase curves for 8/4 resonance.

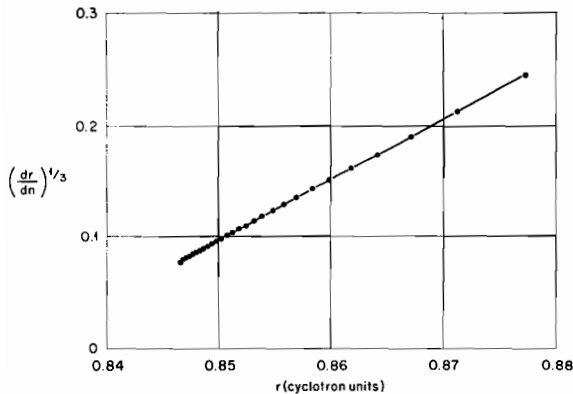


Fig. 232. Rate of growth of radial amplitude with radius, along an asymptote in the phase plot  $dr/dn = C(r - r_0)^3$ .

out to the right along the asymptote shown. They are curling in from above and from below. At this particular  $\theta$  the asymptote leads to essentially pure radial growth. To give you an idea of the size of the picture, the maximum amplitude corresponds to about 50 cm, and as noted before the mean radius is about 500 centimeters. Thus very large radial amplitudes are obtained in this manner.

The next thing we did was to analyze the behavior at one particular orbit which follows quite close to the asymptote. We wanted to find out how large the growth rates were for this orbit. We took the successive  $r$ -values, for that particular orbit as obtained from the computer, and by differencing these values calculated a derivative. Taking the cube root of that derivative and just simply plotting it against the  $r$ -values we should obtain a straight line. As you can see in Figure 232, we do, indeed, obtain a fairly good straight line, showing that the growth rate as anticipated is proportional to the cube of the amplitude. When this line is extrapolated back down it does hit fairly close to the equilibrium orbit, and from its slope we can determine the growth rate constant.

In Figure 233 we used the data from Figure 232 to determine the growth-rate constant, which I call  $C$  here. We determined from integrating the little equation shown the "lifetime,"  $\Delta n$ , of the particle, that is, if started out with a certain initial amplitude  $A_0$ ,  $\Delta n$  is the number of turns the particle will make before its amplitude becomes infinite. At the bottom of the figure there is a small table showing the effect of the nonlinearity along the asymptote. You can see that for 1 cm initial amplitude the particle will last in that orbit for 1,000 turns. Of course, by that time it would have accelerated past the resonance. On the other hand, you see that for 10 cm initial amplitude it would last only a little over 10 turns.

ALONG ASYMPTOTE:

$$\frac{dA}{dM} = CA^3; C = 173.$$

$$\Delta n = \frac{1}{2CA_0^2}$$

$A_0(\text{cm})$	0.1	1.0	2.0	5.0	10.0	20.0
$\Delta n$	$10^5$	$10^3$	260.	41.7	10.4	2.6

(cyclotron unit = 600 cm)

Fig. 233. Determination of the growth-rate constant, C.

INTEGRAL RESONANCE FIELD BUMP

$$\delta B_z = \xi r^2 \sin(2\theta + \gamma)$$

$$\xi = \epsilon \bar{B}(\bar{r})/\bar{r}^2$$

$$\epsilon = 10^{-3}$$

ACCELERATION:  $10^{-3} \text{ mc}^2/\text{turn}$

4 RF gaps

Fig. 234. Introduction of field bump.

Thus it can be seen that if one had a mechanism for building up the radial amplitudes so that this nonlinear driving force took appreciable effect, one could in principle get very large turn separations, clear a septum, and get the beam deflected.

Next, we decided to make some prototype beam deflection runs of a semi-quantitative nature. We had to adapt our calculations to fit the restrictions of the computer. Figure 234 shows the field "bump" which was added in a form dictated by the computer code. The strength of this bump,  $\epsilon$ , was chosen to be  $10^{-3}$  of the average field at that particular radius. The value of gamma was selected so that the field bump would act in such a way as to drive the particles on each successive revolution further out along the asymptote described above. For these runs we set up the computer for an acceleration rate of  $10^{-3}$  which corresponds to about 1-Mev/turn.

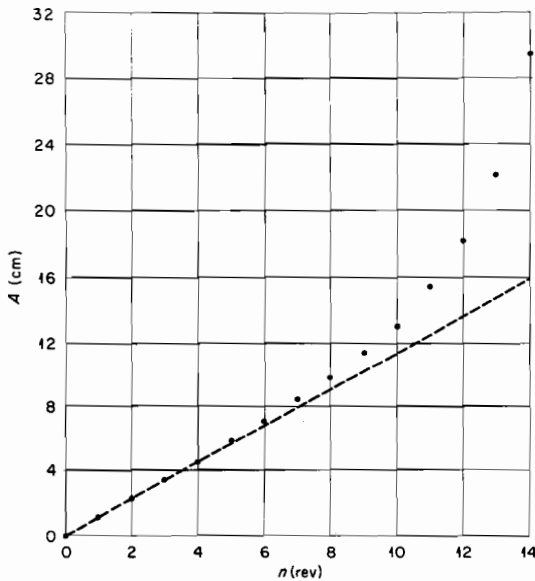


Fig. 235.  $8/4$  resonance driven by  $\epsilon \bar{B} \cos 2\theta$  ( $\epsilon = 10^{-3}$ ).

We started a particle off on the equilibrium orbit 16 revolutions before the resonance. This 16 revolutions represents in a certain sense the effective half-width of the integral resonance as a result of the acceleration rate. In Figure 235 we show the results of this orbit run. In this figure we have plotted the radial displacement in centimeters as a function of the number of revolutions. Here we see that the particle starts out on the equilibrium orbit, and the jumps on successive turns are initially linear, which is what one would expect if the field bump were active all by itself. One can see as the amplitude gets larger the nonlinearity takes over and the points rise above the straight line. The last point, which can't be shown, is so high (54 cm) it just wouldn't fit on the curve. This

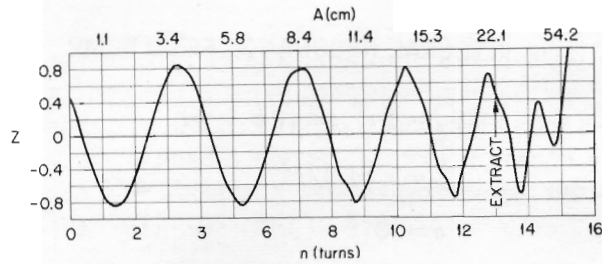


Fig. 236. Effect of  $\nu_r = 2 \nu_z$  resonance on axial motion during extraction.

result indicated to us that the combination of the integral resonance force plus the nonlinearity would mesh together and produce the large turn separation required for beam deflection.

The next thing that we had to examine was axial stability which is, of course, a very serious problem. We repeated the above orbit run, putting in a small axial amplitude, that is, starting the particle slightly off the median

plane in order to see what happened to the axial motion. In Figure 236 are the results of this orbit run. The axial displacement was recorded at intervals of once per sector and the smooth curve shown in this figure was obtained from these points plotted as a function of the number of turns. Also shown at the top of this figure is the corresponding radial amplitude which goes from very small values up to 54 centimeters. If one looks at the axial motion one can clearly see the frequency increasing. The axial frequency starts initially at 0.25 and increases to unity. When it reaches this value, the axial motion finally goes haywire, as can also quite readily be seen. This is the result of the action of the coupling resonance  $\nu_r = 2 \nu_z$  and the fact that the radial amplitude gets quite large.

On the basis of the above results we decided that it was necessary to terminate this beam deflection process at the 13th turn. As can be seen (Fig. 236), beyond this point the axial instability becomes unbearable. Next we made a more complete series of orbit runs to construct a set of phase plots from which the behavior of the beam as a whole could be determined.

First, we have in Figure 237 the phase plots for the radial motion, the fact that the radial amplitude gets quite large. These plots were constructed from eight orbit runs starting with initial conditions equally spaced around an invariant ellipse (eigen ellipse) with a radial amplitude of 0.5 cm. This is the ellipse which is shown farthest to the left in the figure. The computer stores the  $(r, p_r)$  values obtained on successive turns for all these orbits. It then calculates a large number of points on a smooth closed curve which will pass through the eight given points for each turn. The data for all these ellipses and distorted ellipses are then rearranged and plotted by the computer in sixteen separate pictures. These pictures are then pasted together to form the large, detailed figure shown. All this work is done entirely by

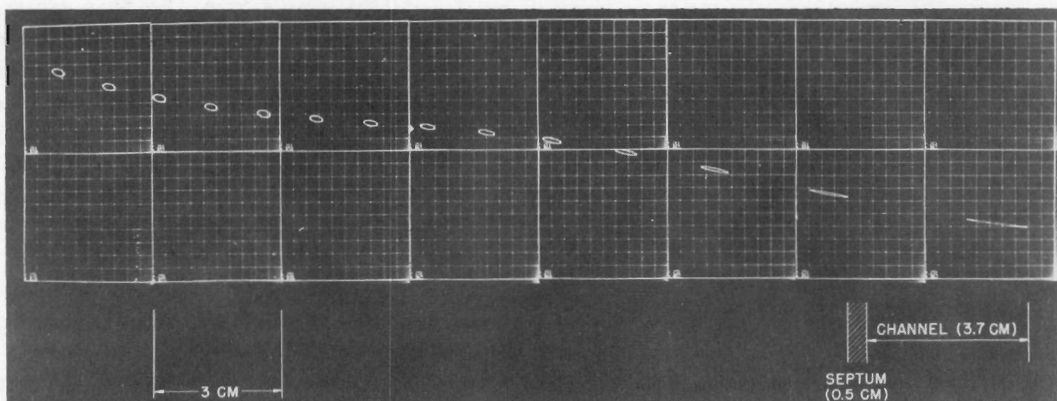


Fig. 237. Motion of invariant ellipses in phase space during extraction ( $\theta = 0$ ).

the computer through an ingenious code for which we are indebted to our talented coder, Miss Thelma Arnett.

We can see how the integral resonance field bump displaces the ellipse to the right initially at a uniform rate (Fig. 237). As the displacement grows, the nonlinearity takes hold and the displacement rate increases, and as a result the ellipses become flattened and elongated (maintaining constant area). Here we have also shown some approximate indication of what one would expect for a septum and a channel. As a result of this work we have a fairly clear idea of the radial motion of the beam during the deflection process.

The phase plots obtained for the axial motion are shown in Figure 238. As can be seen there are four very similar sets of these phase plots. The initial conditions for the corresponding radial motion were chosen to be the  $(r, p_r)$  values at the phase ellipse shown in the previous slide, which explains why we have four sets of axial phase plots here. For each set of axial phase plot runs we chose eight initial  $(z, p_z)$  values equally spaced about an invariant ellipse with an amplitude of 5 cm. Thus, a total of 32 orbit runs were for this figure. The method of construction was the same as that described just above.

Inspection of these phase plots shows several interesting results. Reading from left to right we have the phase plots for the thirteen successive turns during the deflection process. As can be seen the shape of these plots changes drastically; this we can account for as an AG effect from the coupling resonance plus the accompanying accelerated radial growth. The important result to note is the very good overlap of the four sets of phase plots. This implies that the coupling resonance, though quite active, will not appreciably disturb the optical quality of the beam during deflection (provided the beam is deflected at this point, that is, the 13th turn). This is a very encouraging result. We should also remark here that the feedback of the axial motion into the radial motion due to the coupling is not significant since the radial motion is completely dominated by the nonlinear resonance.

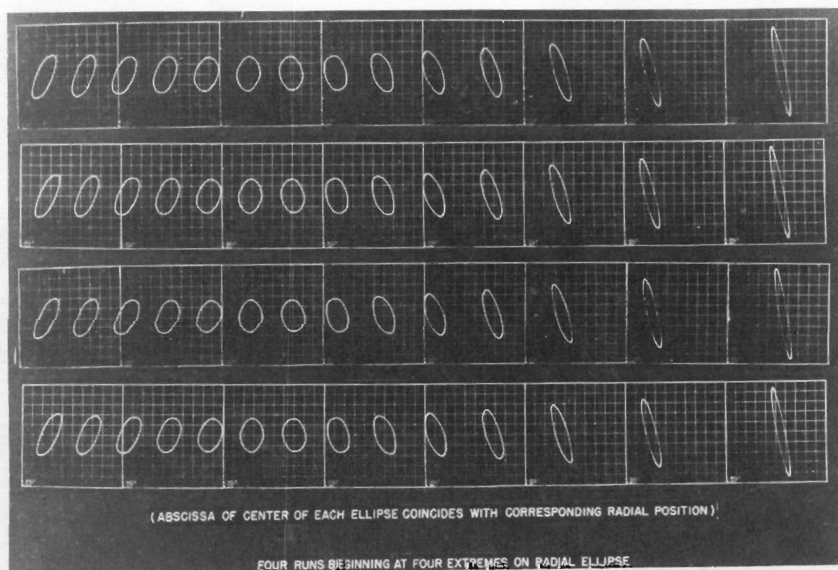


Fig. 238. Behavior of axial invariant ellipses in phase space during extraction.

These then are the results of our calculations testing this deflection scheme for the big cyclotron. The results are encouraging and similar investigations for medium energy machines should certainly be undertaken.

The efficiency of a beam deflection system will, of course, depend on many factors. In this connection, one should consider the possibility of an ideal, "programmed" machine, which has now, we feel, become feasible. In such a machine conditions near the ion source as well as the r-f voltage and waveform are sufficiently well controlled so that every beam pulse follows virtually the same path through the machine. Under these conditions one could expect to achieve nearly 100% efficiency in beam extraction.

In conclusion, I should like to express my gratitude to T. A. Welton for his very considerable help in this work.

JUDD: You gave the simplified equation containing terms pertaining just to the nonlinear resonance. Essentially to couple the differential equations. In carrying out the analysis which you have described was this done with orbit codes which are essentially rigorous? As for high-order terms, were they done analytically with these approximate equations?

GORDON: These are done with real orbit codes which treat analytical forms of the fields.

JUDD: They were such large displacements that I would not think the approximate equation would do.

GORDON: That is right. The approximate equation neglects high-order terms and predicts that the asymptote is straight whereas you can see in Figure 231 that the asymptote curves around.

JUDD: That asymptote sort of started to turn around, which indicated that there are higher-order terms which tend to make it stable.

GORDON: But, of course, this occurred at over 50 cm, which was just too large to worry about. If stability sets in up there, it is too late for anything anyhow.

BLOSSER: What was plotted in the last slide you showed? This was an axial phase plot of some sort.

GORDON: What you are worried about is that the plots should, of course, sit one on top of the other, but they don't. I had originally intended that these four sets of phase plots would sit right under the radial phase plot of Figure 237, right underneath it would be the axial phase plot pertaining to the same term. Unfortunately, it would not go on one slide, but we have it on two slides; so the horizontal spacing between the plots is just an indication of what the radial growth is, you see. But each one of these is centered at  $z = 0$ ,  $p_z = 0$ , and displacement has no significance as far as axial motion is concerned.